**Preprints of the 21st IFAC World Congress (Virtual)**
**Berlin, Germany, July 12-17, 2020**

# Comparisons of robust methods on feedback linearization through experimental tests ⋆

**Lucas Oliveira** * **Anderson Bento** * **Valter J. S. Leite** *
**Fernando Gomide** **

* *Department of Mechatronics Engineering, CEFET–MG, R. Álvares Azevedo, 400,* 35503-822*, Divinópolis, MG, Brazil (e-mail: lqsoliveira@cefetmg.br, bentoavb@gmail.com, valter@ieee.org).*
** *School of Electrical and Computer Engineering, University of Campinas, Av. Albert Einstein, 400,* 13083-852 *Campinas, SP, Brazil (e-mail: gomide@dca.fee.unicamp.br)*

**Abstract:** The feedback linearization is a powerfull nonlinear method based on the principle of canceling the nonlinearities of the system model. However, if the model differs from the real system, the feedback linearization is prone to fail. Several studies look to provide robustness to the feedback-linearized system, but we note a lack of evaluation among such approaches under similar conditions in practical systems. This work contributes to filling such a gap by comparing the performance of three recent approaches proposed to robustify feedback linearization loops. Therefore, we design controllers based on the robust multi-inversion (RMI), the robust dynamic inversion (RDI), and the robust granular feedback linearization (RGFL), and evaluate them through real-time experiments. The test process consists of a nonlinear surge tank where the level must be controlled. Two experiments are performed to evaluate the controllers in the tracking and regulation modes when the system is subjected to disturbances. Classical quantitative indexes evaluate the performance of the closed-loop system. The experimental tests indicate that the RGFL controller outperforms the other approaches in both regulation and tracking.

*Keywords:* Feedback linearization, robust control, granular computing, evolving systems, adaptive control.

## 1. INTRODUCTION

The feedback linearization is a nonlinear method that has been receiving increasing attention in recent years, both for its theoretical importance as well as for its impact in various fields of application. One general drawback of feedback linearization is that the method requires an exact cancellation of the nonlinearity to achieve the system linearization (Ko et al., 1999). This characteristic does the method susceptible to fail whenever there are model mismatches or neglected dynamics (Oliveira et al., 2019b). In practice, neglected dynamics and time-varying uncertainties affect industrial processes and machines (Dinh et al., 2018). Therefore, robust and adaptive control schemes became fundamental, and investigations conducted during the last decades have substantially contributed to improving the effectiveness control loop (de Jesús Rubio, 2018). For instance, Franco et al. (2006) present a robust feedback linearization scheme where the McFarlane-Glover $H_\infty$ controller (McFarlane and Glover, 1992) is associated with the feedback linearized closed-loop system, improving the results in (Guillard and Boulès, 2000). The effect of modeling errors is counteracted in (Lavergne et al., 2005), adding an extra loop in a framework called robust-multi inversion (RMI). Such an approach motivated a similar scheme investigated in (Oliveira et al., 2015), where a signal given by the time-integral of the linear control signal is added to the control signal to compensate for the model mismatches. Moreover, the controller gains are determined by a differential evolution (DE) algorithm (Chakraborty, 2008, Chap. 2) jointly with a set of linear matrix inequalities (LMIs), ensuring the robust stability of the closed-loop system. Recently, Oliveira et al. (2019a) introduced a novel robust granular feedback linearization (RGFL) controller that gives a compensation control signal. Such compensation is delivered by the evolving participatory learning (ePL) algorithm (Lima et al., 2006), allowing online estimates of the uncertainties of the controlled process and the respective counteraction of their effects in the control-loop. Note, however, that there are no experimental comparisons of these novel methods in the literature. Such a step is welcome because some theoretical methods may degenerate their performance under practical issues such as measurement noise, model-mismatches, and external disturbances.

In this paper, we propose to evaluated the performance of the closed-loop using the RMI, RDI, and RGFL ap-

⋆ This work was partially supported by the Federal Center of Technological Education of Minas Gerais (CEFET-MG) grant 10673/2018, and the Brazilian National Council for Scientific and Technological Development (CNPq) grants 305906/2014 − 3 and 311208/2019 − 3.

proaches. These control schemes are used to regulate the level in a real nonlinear surge tank system. Additional time-varying income water flows disturb the controlled level during the experimental tests, yielding realistic conditions for industrial purposes. We use classical control indexes, such as integral absolute error (*IAE*), the integral of time-weighted absolute error (*ITAE*), root mean square error (*RMSE*), and the euclidean norm of the control signal ($\|u\|_2$) to quantify and compare the controllers performance. The results suggest that the RGFL outperforms the remainder control schemes.

This paper is structured as follows: In Section 2, it is presented the feedback linearization method and stated its fragility concerning the model-mismatches. In Section 3, a short revision of the robust methods focused in this paper is shown. Experimental setup and test results are given in Section 4. The concluding remarks are presented in Section 5.

## 2. PROBLEM STATEMENT

Consider the class of nonlinear system depicted by:

$$x^{(n)} = f(\mathbf{x}) + g(\mathbf{x})u;\ y = C_c\mathbf{x} \tag{1}$$

where $\mathbf{x} \in \mathbb{R}^n$ is the system state vector, $x^{(n)}$ is the $n$-th derivate of the state, $u \in \mathbb{R}$ is the control signal, $y \in \mathbb{R}$ is the output system, $C_c \in \mathbb{R}^{1\times n}$, $f(\cdot)$ and $g(\cdot)$ are smooth functions defined in a domain $\mathrm{D} \in \mathbb{R}^n$ yielding the vector fields $f(\cdot) : \mathrm{D} \to \mathbb{R}^n$ and $g(\cdot) : \mathrm{D} \to \mathbb{R}^n$. The system (1) can be linearized by feedback action, if some conditions such as smooth distribution, involute properties, and linear independence between the vectors fields are attempted (Khalil, 2002). In such case, there is a nonlinear state feedback control law given by:

$$u = g(\mathbf{x})^{-1}\left[v - f(\mathbf{x})\right], \tag{2}$$

which yields, for a relative degree $r$, a linear dynamics between the control signal $v$ and the output $y$ as follows: $x^{(n)} = y^{(r)} = v$, for all $\mathbf{x} \subset \mathrm{D}$ and $g(\mathbf{x}) \neq 0$.

Although, it is clear that the mechanism of linearization through state feedback linearization involves the exact cancellation of nonlinearities. Consequently, it relies on a rather precise description of nonlinear functions (Khalil, 2002). In practice, industrial processes and complex systems as an airplane, robotics system, and transport system are affected by constant and time-varying uncertainties or parasitic dynamics (Khalil, 2002). For instance, assume that the vector fields $f(\cdot)$ and $g(\cdot)$ are affected by parametric and additives uncertainties, as follows:

$$\begin{aligned} f(\mathbf{x}) &= f_n(\mathbf{x}) + \Delta f(\mathbf{x}), \\ g(\mathbf{x}) &= g_n(\mathbf{x}) + \Delta g(\mathbf{x}), \end{aligned} \tag{3}$$

where $f_n(\cdot)$ and $g_n(\cdot)$ are the precise known nonlinear functions, and $\Delta f(\cdot) = \Delta f$ and $\Delta g(\cdot) = \Delta g$ are the modeling error or additives uncertanties. Pluging (3) in (1), we have:

$$x^{(n)} = f_n(\mathbf{x}) + g_n(\mathbf{x})u + d(\mathbf{x},u) \tag{4}$$

with $d(\mathbf{x},u) = \Delta f(\mathbf{x}) + \Delta g(\mathbf{x})u$ is an exogenous disturbance on the closed-loop. Using the control law (2) where the control signal is computed as $u = g_n(\mathbf{x})^{-1}\left[v - f_n(\mathbf{x})\right]$, the closed-loop system is given by: $x^{(n)} = y^{(r)} = v + d(\mathbf{x},u)$. Assuming the linear control law $v$ defined by a state feedback control law, $v = \mathbf{K}\mathbf{x}$, where $\mathbf{K}$ is the state feedback gain designed, for instance, through placement pole or linear quadratic regulator (LQR) method. The closed-loop system can be rewritten in the following state-space form:

$$\dot{\mathbf{x}} = A_c\mathbf{x} + B_c d(\mathbf{x},u) \tag{5}$$

with $A_c = \begin{bmatrix} 0 & 1 & 0 & \cdots & 0 \\ 0 & 0 & 1 & \cdots & 0 \\ \vdots & \vdots & \vdots & \ddots & \vdots \\ k_n & k_{n-1} & k_{n-2} & \cdots & k_1 \end{bmatrix}$ and $B_c = \begin{bmatrix} 0 \\ 0 \\ \vdots \\ 1 \end{bmatrix}$.

## 3. ROBUST CONTROL SCHEME

In this section, we briefly review three recent control schemes named robust multi-inversion (RMI), robust dynamic inversion (RDI), and robust granular feedback linearization (RGFL). Theses methods seek to improve the robustness of the feedback linearization control method. In all control strategies evaluated in this paper, looking for adding an external compensation loop at the feedback linearization loop, in order to mitigate the effects caused by the exogenous disturbance, $d(\mathbf{x},u)$, on the closed-loop system. These methods have similar control structures, as shown in Figure 1, to solve the tracking problem, where $\mathbf{r}(t)$ is infinity diferenciable function to desired trajectory and $\mathbf{e}(t) = \mathbf{r}(t) - \mathbf{x}(t)$ is the tracking error vector. However, each technic uses a particular mechanism to compute the compensation signal, $u_c$.

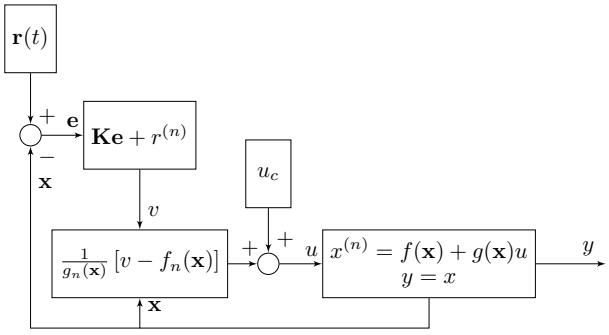


Fig. 1. General robust control scheme.

### *3.1 Robust Multi-Inversion*

The robust multi-inversion (RMI) method was developed by Lavergne et al. (2005). The proposed method uses a model-error to improve robustness of the feedback linearized closed-loop system (5). An additional control signal is added to linear control law $v$, as follows: $\tilde{v} = v + \Delta_{RMI}$, where $\tilde{v}$ is the linear control signal with correction, and $\Delta_{RMI}$ is the compensation signal, given by:

$$\Delta_{RMI} = \mathbf{K}_{RMI} \int \left(y^{(r)}_{RMI} - y^{(r)}\right) dt, \tag{6}$$

$$y^{(r)}_{RMI} = f_n(\mathbf{x}) + g_n(\mathbf{x})u - \Delta_{RMI}, \tag{7}$$

where $\mathbf{K}_{RMI}$ is the RMI gain, and $y^{(r)}_{RMI}$ is the observed output model error. By plugging (7) into (4) and considering the uncertainties (3) in (6), we have:

$$\Delta_{RMI} = \mathbf{K}_{RMI} \int \left(d(\mathbf{x},u) - \Delta_{RMI}\right) dt. \tag{8}$$

It is worth to say that the authors in (Lavergne et al., 2005) do not provide a method to compute the the control

gain $\mathbf{K}_{RMI}$. Instead, they give robust closed-loop analysis procedure based on convex methods. Therefore, the control law (2) can be rewritten as follows: $u(\mathbf{x},\Delta_{RMI}) = g_n(\mathbf{x})^{-1}\left[v + \Delta_{RMI} - f_n(\mathbf{x})\right]$. Note that, in this approach the compensating control signal presented in Figure 1 corresponds to $u_c = g_n(\mathbf{x})^{-1}\Delta_{RMI}$. Considering a state feedback control, with $v = \mathbf{K}\mathbf{x}$, the dynamics of the closed-loop is governed by: $\dot{\mathbf{x}} = A_c\mathbf{x} + B_c\left(d(\mathbf{x},u) - \Delta_{RMI}\right)$, which yields in $\Delta_{RMI} \to d(\mathbf{x},u)$ as $t \to \infty$, consequently, $(d(\mathbf{x},u) - \Delta_{RMI}) \to 0$ when $t \to \infty$.

### *3.2 Robust Dynamic Inversion*

The robust dynamic inversion (RDI) controller was motivated by the work (Lavergne et al., 2005) and investigated by Oliveira et al. (2015). This approach uses the difference between the linear control signal and the system output to improve robustness in linearizable feedback systems. Thus, the compensation signal is computed by: $\Delta_{RDI} = \mathbf{K}_{RDI}\left(\int_0^t v dt - y\right)$, where $\mathbf{K}_{RDI}$ is the compensating gain of the RDI topology. It is added to linear control signal yielding in the control law given by:

$$u(\mathbf{x},\Delta_{RDI}) = g_n(\mathbf{x})^{-1}\left[v + \Delta_{RDI} - f(\mathbf{x})\right], \tag{9}$$

where the compensation control signal related with Figure 1 is given by $u_c = g_n(\mathbf{x})^{-1}\Delta_{RDI}$. Applying (9) in (4), it results in

$$x^{(n)} = v + \mathbf{K}_{RDI}\left(\int_0^t v dt - y\right) + d(\mathbf{x},u), \tag{10}$$

and the closed-loop dynamics can be written in a state-space form as follows:

$$\begin{aligned}\dot{\mathbf{x}} = &\left(A_c - B_c\mathbf{K}_{RDI}C_c\right)\mathbf{x} \\ &+ B_c\left(v + \mathbf{K}_{RDI}\int_0^t v dt + d(\mathbf{x},u)\right).\end{aligned} \tag{11}$$

A new state variable is defined as $\hat{\mathbf{x}} \in \mathbb{R}^{n+1}$, where $\hat{\mathbf{x}} = \left[\int_0^t v dt \ \ \mathbf{x}^T\right]^T$. By considering the state feedback control law $v = \mathbf{K}\mathbf{x}$, the system (11) can be rewritten as:

$$\begin{bmatrix} v \\ \dot{\mathbf{x}} \end{bmatrix} = \underbrace{\begin{bmatrix} \mathbf{0} & \mathbf{K} \\ B_c\mathbf{K}_{id} & A_c - B_c\mathbf{K}_{id}C_c + B_c\mathbf{K} \end{bmatrix}}_{A_0}\hat{\mathbf{x}} + \underbrace{\begin{bmatrix} \mathbf{0} \\ B_c \end{bmatrix}}_{B_0} d(\mathbf{x},u). \tag{12}$$

Assuming that the uncertainty $d(\mathbf{x},u)$ is bounded, that is, $d(\mathbf{x},u)^T d(\mathbf{x},u) = \delta\mathbb{F}\hat{\mathbf{x}}$, where $\mathbb{F} \in \mathbb{R}^{(n+1)\times(n+1)}$ is given by, $\mathbb{F} = \begin{bmatrix} \mathbf{0} & \mathbf{0} \\ \mathbf{0} & 1 \end{bmatrix}$. The closed-loop stability is ensured by the following theorem:

*Theorem 1.* Consider the feedback linearized and compensated system (12). If there exist a symmetric positive definite matrix $\tilde{P} \in \mathbb{R}^{(n+1)\times(n+1)}$ and a real scalar $\delta > 0$, such that,

$$\begin{bmatrix} A_0^T\tilde{P} + \tilde{P}A_0 + \delta\mathbb{F} & \tilde{P}B_0 \\ \star & -1 \end{bmatrix} < 0 \tag{13}$$

is feasible, then the system is exponentially stable with a Lyapunov function given by $V(\hat{\mathbf{x}}) = \hat{\mathbf{x}}^T\tilde{P}\hat{\mathbf{x}}$.

The proof of Theorem 1 can be found in (Oliveira et al., 2015).

### *3.3 Robust Granular Feedback Linearization*

The robust granular feedback linearization (RGFL) control scheme was introduced by Oliveira et al. (2019b). Similar to RMI and RDI methods, this approach uses the evolving participatory learning (ePL) algorithm (Pedrycz and Gomide, 2007, Chap. 13) to improve robustness in the feedback linearization loop. This algorithm is applied to estimate the disturbance, $\hat{d}(\mathbf{x},u)$, present on the closed-loop system (5), and from such an estimate a control compensation signal is computed. Therefore, the compensating control signal is designed to mitigate the effects of the disturbances on the closed-loop and is added in the nonlinear control signal as follows: $u_c = -g_n(\mathbf{x})^{-1}\hat{d}(\mathbf{x},u)$. In this case, the control law (2) is rewritten as

$$u = \underbrace{g_n(\mathbf{x})^{-1}\left[v - f_n(\mathbf{x})\right]}_{u_n} - \underbrace{g_n(\mathbf{x})^{-1}\hat{d}(\mathbf{x},u)}_{u_c} \tag{14}$$

where $u_n$ is the control signal computed by (2) using the known functions $f_n(\mathbf{x})$ and $g_n(\mathbf{x})$. The RGFL controller uses functional fuzzy rules of the form:

$$\textbf{IF } \mathbf{z}^k \text{ is } \mathcal{V}_i \textbf{ THEN } \hat{d}_i^k(\mathbf{x},u) = \gamma_i^k\xi^k \tag{15}$$

where $\mathbf{z}^k = \left[(\mathbf{x}^k)^T \ e_1^k\right]^T \in [0,1]^{n+1}$ is the input data, $e_1^k$ is the output tracking error, $\mathcal{V}_i$ is the $i$-th antecedents rules, $\hat{d}_i^k(\mathbf{x},u)$ is the estimated value by the $i$-th rule, $\gamma_i^k \in \mathbb{R}^{n+1}$ is the consequents of the rule and $\xi^k$ is a vector parameters given by: $\xi^k = \left[\left(\mathbf{z}^k\right)^T \ 1\right]^T$. The fuzzy rule set is online updated by using granular computing concepts. In this sense, each rule is depicted by a cluster center, $\mathbf{v}_i \in [0,1]^{n+1}$, corresponding to a modal value of Gaussian membership functions of the antecedent fuzzy set: $\mu_i^k\left(\mathbf{z}^k\right) = e^{-\frac{\|\mathbf{z}^k - \mathbf{v}_i^k\|^2}{\sigma}}$, where $\mu_i^k\left(\mathbf{z}^k\right)$ is the firing degree of the $i$-th fuzzy rule, $\|\cdot\|$ is the Euclidian norm, and $\sigma$ is the spread or influence zone of the Gaussian function. Once the algorithm is initialized, at each processing step, the participatory learning mechanism verifies if a new cluster must be created, if a current rule should be updated to accommodate the new sample data input, or if redundant clusters should be deleted (Pedrycz and Gomide, 2007). This mechanism starts computing the compatibility measure $\rho_i^k \in [0,1]^{c^k}$ and arousal index $a_i^k \in [0,1]^{c^k}$ for $i = 1, \cdots, c^k$, as follows:

$$\rho_i^k = 1 - \frac{\|\mathbf{z}^k - \mathbf{v}_i^k\|}{\sqrt{n+1}}, \tag{16}$$

$$a_i^{k+1} = a_i^k + \beta\left(1 - \rho_i^k - a_i^k\right), \tag{17}$$

where $c^k$ is the number of rules at $k$-th step, and $\beta \in [0,1]$ is the arousal rate. Thus, if the smallest arousal index value is bigger than the threshold $\tau \in [0,1]$, that is, $\text{argmin}_{i\,=\,1,\,\cdots\,,\,c^k}\left\{a_i^{k+1}\right\} > \tau$, then a new cluster is created, $\mathbf{v}_{c^k+1} = \mathbf{z}^k$. Otherwise, the cluster center most compatible with the current input data is updated by:

$$\begin{aligned} s &= \underset{j\,=\,1,\,\cdots\,,\,c^k}{\text{argmax}}\left\{\rho_j^k\right\}, \\ v_s^{k+1} &= v_s^k + \alpha\left(\rho_s^k\right)^{1-a_s^{k+1}}\left(\mathbf{z}^k - \mathbf{v}_s^k\right). \end{aligned} \tag{18}$$

where $\alpha \in [0,1]$ is a learning rate. Note that, the output of the $i$-th rule (15) is an affine function that describes a local linear model, which is governed by the relation between the

consequents rules ($\gamma_i^k$) and the states of the linear model, given by ($\xi^k$). Moreover, the consequent vector is updated by a recursive method, for instance, using the recursive least square ($RLS$) method (Ljung, 1999).

The participatory learning mechanism also verifies if redundant clusters have been created. In this way, the compatibility between clusters centers are computed using:

$$\rho_{ij}^k = 1 - \frac{\|\mathbf{v}_i^k - \mathbf{v}_j^k\|}{\sqrt{n+1}} \tag{19}$$

where $i = 1, \cdots, c^k - 1$ and $j = i+1, \cdots, c^k$. Thus, if $\rho_{ij}^k \geq \lambda$, where $\lambda \in [0,1]$ is a threshold, then the cluster center $\mathbf{v}_j$ is declared redundant, and it is removed from the current cluster structure. Consequently, the corresponding fuzzy rule is also deleted from the fuzzy rule set. Otherwise, the current fuzzy rule set remains as it is.

The output of the RGFL controller is computed by a weighted average of the individual local linear model, that is,

$$\hat{d}^k(\mathbf{x},u) = \frac{\sum_{i=1}^{c^k} \mu_i^k \hat{d}_i^k(\mathbf{x},u)}{\sum_{i=1}^{c^k} \mu_i^k}. \tag{20}$$

Details of the RGFL algorithm, please see (Oliveira et al., 2019b).

## 4. PERFORMANCE EVALUATION

We run real-time experiments to control the level in a nonlinear surge tank to evaluate the achieved closed-loop performance of each method described in Section 3. The level control problem in a surge tank is a benchmark used by many authors (Banerjee et al., 2011; Andonovski et al., 2018; Oliveira et al., 2019a) to evaluate the robust feedback linearization approach. In this paper, we use the nonlinear surge tank system depicted in Figure 2. This

Fig. 2. Surge tank system.

system is composed of four tanks with a nominal capacity of the 200 $l$ each, and two water reservoirs with a nominal capacity of 400 $l$ each. To measure the level, each tank is equipped with a pressure sensor model $26PCBFA6D$. The control system responds to the control signal through two three-phase 1 HP hydraulic pumps commanded by two WEG CFW09 inverters. The controller runs in a low-cost computer (Raspberry Pi 3) that take the measures performed and stored in a Simatic S7-300 programmable logic controller (PLC). The computer and the PLC are connected via Ethernet protocol, and a Python based interface allows to program the controller (Sousa et al., 2018). In this paper, we are interested in controlling the level of the isolated tank $T3$, which dynamics is given by:

$$\dot{h} = \frac{17.25u}{A(h)} - \frac{7.65h + 301.65}{A(h)} + \frac{d(\mathbf{x},u)}{A(h)} \tag{21}$$

where $h \in [8,\ 70]$ is the level ($cm$), $u \in [0,\ 100]$ is the control signal sent to the pump (%), and $A(h)$ is the cross-sectional area of the tank ($cm^2$) given by $A(h) = 1556.82 - 1349.1948\cos(2.5\pi\theta)e^{\frac{-\theta^2}{0.605}}$ with $\theta = 0{,}01(h-8) - 0{,}4$. The variable area of this tank comes from a designed solid in expanded polystyrene, put inside the tank. The tank model (21) has the form of the nonlinear system (1), with $f(\mathbf{x}) = -\frac{7.65h+301.65}{A(h)}$ and $g(\mathbf{x}) = \frac{17.25u}{A(h)}$. Thus, it can be feedback linearized by the control law (2), yielding:

$$u^k = \frac{A\left(h^k\right)}{17.25}\left[v + \frac{7.65h^k + 301.65}{A\left(h^k\right)}\right]. \tag{22}$$

Moreover, we use the state feedback control law, $v$, as follows: $v = -0.05e^k + \left(\frac{r^k - r^{k-1}}{T}\right)$, where $e^k = r^k - h^k$ is the tracking error, and $T = 1\ s$ is the sampling time, which is small enough to keep the continuous-time approximation. Note that, all methods evaluated in this paper use the same linear control law. To compute the compensation signal, the approaches RMI, RDI, and RGFL use respectively (8), (9) and (14). The RGFL functional fuzzy rules is defined as

$$\textbf{IF } z^k \text{ is } \mathcal{V}_i \textbf{THEN } \hat{d}_i^k(\mathbf{x},u) = \gamma_i^k \left[z^k\ 1\right]^T \tag{23}$$

where, $z^k = \left[h^k\ e^k\right]^T$ the consequents $\gamma_i^k \in \mathbb{R}^3$ are computed using the RLS method.

Before running the experiments, simulations were implemented with the system model and the parameters of the RGFL controller were chosen by trial and error following the guidelines found in (Pedrycz and Gomide, 2007, Chap. 13). All parameters values are in the range [0, 1]. In particular, we set $\alpha = 0.0075$, $\beta = 0.0001$, $\tau = 0.001$, $\lambda = 0.875$, and $\sigma = 0.0025$. Besides that, the RGFL controller uses forgetting factor $\zeta = 0.98$ and gains $K_p = 1.25$ and $K_i = \frac{K_p}{100}$. Input data are normalized using $h_{\max} = 70cm$ and $e_{\max} = 35cm$. All experimental tests run using the $\mathbf{K}_{RMI} = \mathbf{K}_{RDI} = 0.2495$ as suggest in (Franco et al., 2016).

Two experiments were run to evaluate the controller approaches on the tracking and on the regulation modes. In the first one we focus on the tracking, where the desired reference $r^k$ is designed as a sequence of smooth steps computed by:

$$r^k = r^{k-1} + \frac{h_0^k - h_0^{k-1}}{1 + e^{-0.15(k - h_0^k - 35)}}, \tag{24}$$

where $k$ is the time-step and $h_0$ taken in the sequence $\{40,\ 50,\ 60,\ 50,\ 40,\ 50,\ 60,\ 50,\ 40,\ 60,\ 40,\ 60,\ 40\}$ in time intervals of 250 $s$. Such a choice, lead to the reference signal shown in dashed line in the top of the Fig. 3. Moreover, we impose a disturbance in the system by increasing the output flow, as follows:

$$d^k = \begin{cases} -2.68h^k - 225.91 & \text{if } t \leq 1000 \\ 127.5\Lambda - 2.68h^k - 225.91 & \text{if } 1000 < t \leq 2000 \\ -2.68h^k - 225.91 & \text{otherwise} \end{cases} \quad (25)$$

where $\Lambda = \left[1 + \cos\left(\frac{\pi}{125}(k - 1000)\right)\right]$. For $t \leq 1000$ and $t > 2000$, the disturbance is equivalent to putting a modeling error in the nonlinear function $f(\mathbf{x})$ about 35%, that is, $f(\mathbf{x}) = 1.35 f_n(\mathbf{x})$. On the other hand, in the interval time $1000 < t \leq 2000$ a time-varying disturbance on the output flow is applied on the system. This procedure was repeated four times with the feedback linearization (EFL) method in cyan line, i.e., with no compensation control signal, and with the three methods RDI (green line), RMI (blue line), and the RGFL (red line). The respective measured signals are in Fig. 3: on the top are the controlled level, in the middle the control signal, and on the bottom the disturbance signal. The reader can note that the level controlled by the RGFL(red line) tracks better the reference signal. We give a quantitative analysis of theses experiments later on.

The second experiment aims to check the performance of the controllers under regulation. Then, we apply a rectangular pulse as a disturbance. In this case, the level system must be regulated at the setpoint, $h = 50\ cm$. We added three flow pulses, each of them with an amplitude of 255 $cm^3/s$ and a duration of 20 $s$. The time-interval between the pulses is 10 $s$. Experimental results are shown in Fig. 4 for each of the controllers EFL (cyan line), RDI (green line), RMI (blue line), and the RGFL (red line). In the top of Fig. 3 is shown the regulated level (top), the control signal (middle), and the disturbance (bottom). The better behavior of the RGFL can be noted, as the level presents less deviation in this case. Such a observation is confirmed by the quantitative indexes presented later on.

From Figures 3 and 4, we can verify that the EFL methods do not reject the effects caused by the raise output flow, which was expected. Spite of that, the remainders of the robust approaches the effects of the disturbances were mitigated. In this case, to the first experiment, we can observe that the RGFL controller reduces the number and amplitude of the overshoots on the closed-loop system. Besides that, in the second experiment, it is verified that the integrate term present on the RMI and IDR methods turn the performance of the closed-loop worse than the performance achieved by the RGFL controller. Moreover, from Figure 3 we can verify that the learning process of RGFL reduces the overshoot amplitude of the output behavior from $t = 2500\ s$ up to $t = 3000\ s$, when is compared with the output behavior from $t = 2000\ s$ up to $t = 2500\ s$. The closed-loop performance was evaluated using the classical control indexes integral of the absolute error ($IAE$), integral of time-weighted absolute error ($ITAE$), root mean square error ($RMSE$), and the euclidean norm of the control signal ($\|u\|_2$). Theses indexes were normalized using, $I_{x,n} = \frac{I_x}{I_{RGFL}}$, and the results are shown in Tables 1 and 2. Therefore, if the index value is higher than one, it's performance is worst than that achieved by the RGFL controller. Otherwise, if the index value is smaller than one, it indicates that the RGFL controller performs worst. From Table 1, we can verify that in general the RGFL controller outperforms the remainder methods. Exceptions are found in the $\|u\|_2$ index, where the EFL method shown the best value, which is expected because this method does not act to mitigate the disturbance effects on closed-loop. Also, the RMI controller achieves a better RMSE performance during the first part of the test, i.e., from $t = 0\ s$ up to $t = 1000\ s$.

Table 1. Performance indexes normalized to RGFL for the first experiment.

| Method | Interval[s] | $IAE$ | $ITAE$ | $RMSE$ | $\|u\|_2$ |
|---|---|---|---|---|---|
| EFL | $0 - 1000$ | 24.41 | 25.69 | 2.31 | 0.85 |
| RMI | | 1.39 | 1.42 | 0.86 | 1.02 |
| RDI | | 1.38 | 1.46 | 1.19 | 1.05 |
| EFL | $1000 - 2000$ | 24.49 | 26.61 | 19.60 | 0.87 |
| RMI | | 2.01 | 2.23 | 1.90 | 1.19 |
| RDI | | 1.87 | 2.03 | 2.04 | 1.20 |
| EFL | $2000 - 2500$ | 26.96 | 33.58 | 14.33 | 0.87 |
| RMI | | 1.34 | 1.19 | 2.09 | 1.23 |
| RDI | | 1.72 | 1.59 | 1.90 | 1.22 |
| EFL | $2500 - 3000$ | 39.92 | 44.28 | 18.47 | 0.84 |
| RMI | | 1.91 | 1.48 | 1.95 | 1.12 |
| RDI | | 2.62 | 2.24 | 2.05 | 1.12 |

Moreover, in the second experiment, we can see from Table 2 that three approaches have almost the same control signal norm (thus, almost the same energy spend), but the RGFL approach outperforms both strategies of control, RMI and RDI, achieving better values of IAE, ITAE and RMSE.

Table 2. Performance indexes normalized to RGFL for the second experiment.

| Method | Interval[s] | $IAE$ | $ITAE$ | $RMSE$ | $\|u\|_2$ |
|---|---|---|---|---|---|
| EFL | $0 - 200$ | 5.65 | 7.03 | 5.96 | 1.13 |
| RMI | | 1.74 | 2.11 | 1.86 | 1.00 |
| RDI | | 1.73 | 2.02 | 1.80 | 1.00 |
| EFL | $200 - 400$ | 8.63 | 8.90 | 9.12 | 1.11 |
| RMI | | 2.13 | 2.27 | 2.46 | 1.00 |
| RDI | | 2.05 | 2.20 | 2.40 | 1.00 |

## 5. CONCLUSION

We have experimentally tested three recent compensation strategies (RDI, RMI, and RGFL) to improve the robustness of the feedback linearization approach. To get more realistic industrial conditions, we introduced constant and time-varying disturbances in all tests. The time to run all algorithms was not an issue for a sample time of 1 $s$, indicating that the can run in standard industrial devices. The experiments suggest that the RGFL strategy, which is based on a participatory learning algorithm, achieves better performance in both regulation and tracking essays than the compared methods. Such a better closed-loop behavior is confirmed by classical quantitative performance indexes, such as IAE, ITAE, RMSE, and $\|u\|_2$. Also, the reader can note from the experimental data, that the RGFL control scheme faster rejects the effects on the closed-loop caused by the disturbances. Consequently, even that RGFL has a more parameters to tune than the other investigated methods, its enhanced performance may justify its choice in high performance processes.

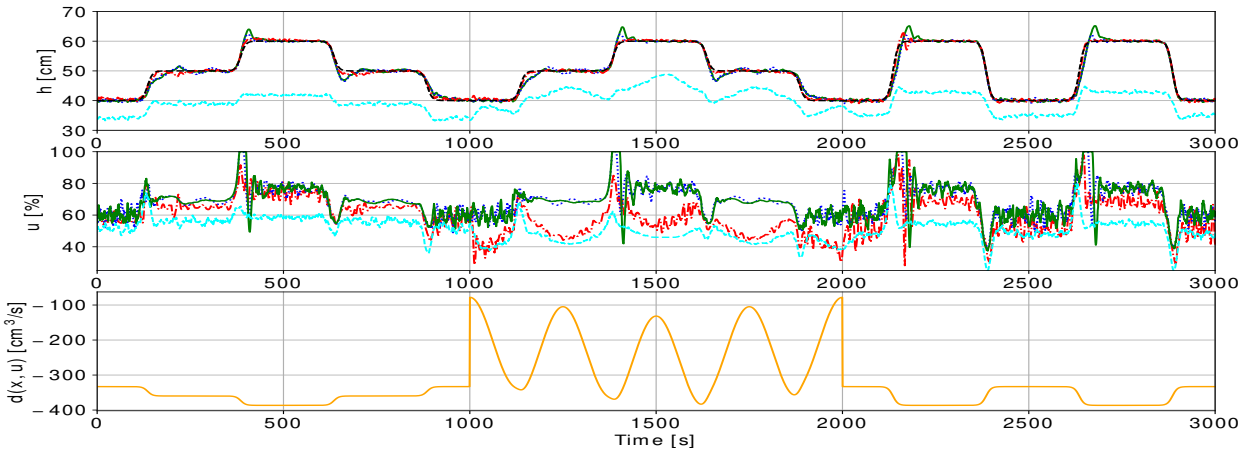


Fig. 3. Surge tank behavior in the first experiment using: EFL method cyan line, RGFL controller red line, RMI controller blue line, RDI controller green line, and the desired trajectory black dashed-line.

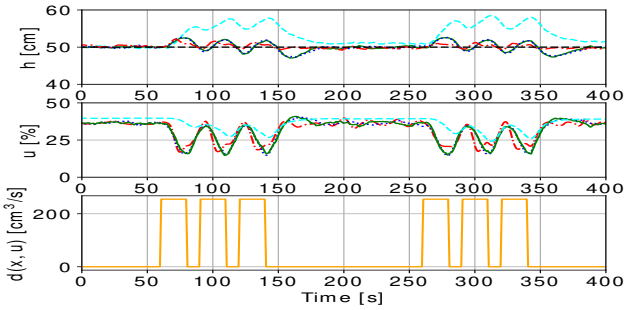


Fig. 4. Surge tank behavior in the second experiment using: EFL method cyan line, RGFL controller red line, RMI controller blue line, RDI controller green line, and the desired trajectory black dashed-line.

## REFERENCES

Andonovski, G., Costa, B., Blažič, S., Škrjanc, I., 09 2018. Robust evolving controller for simulated surge tank and for real two-tank plant. at - Automatisierungstechnik 66, 725–734.

Banerjee, S., Chakrabarty, A., Maity, S., Chatterjee, A., 2011. Feedback linearizing indirect adaptive fuzzy control with foraging based on-line plant model estimation. Applied Soft Computing 11 (4), 3441 – 3450.

Chakraborty, U. K., 2008. Advances in Differential Evolution, 1st Edition. Springer-Verlag, Berlin, Heidelberg.

de Jesús Rubio, J., 2018. Robust feedback linearization for nonlinear processes control. ISA Transactions 74, 155 – 164.

Dinh, T., Marco, J., Yoon, J., Ahn, K., 2018. Robust predictive tracking control for a class of nonlinear systems". Mechatronics 52, 135 – 149.

Franco, A. E. O., Oliveira, L. S., Leite, V. J. S., Outubro 2016. Síntese de ganhos para compensação robusta de sistema linearizados por realimentação. In: Congresso Brasileiro de Automática. Vitória, ES, pp. 2695 – 2700.

Franco, A. L. D., Bourlès, H., De Pieri, E., Guillard, H., 08 2006. Robust nonlinear control associating robust feedback linearization and $H_\infty$ control. Automatic Control, IEEE Transactions on 51, 1200 – 1207.

Guillard, H., Boulès, H., Jun. 2000. Robust feedback linearization. In: Proceedings of the 14th International Symposium on Mathematical Theory of Networks and Systems. Perpignan, France, pp. 1–6.

Khalil, H. K., 2002. Nonlinear systems, 3rd Edition. Prentice-Hall, Upper Saddle River, NJ.

Ko, J., Strganac, T. W., Kurdila, A. J., Mar 1999. Adaptive feedback linearization for the control of a typical wing section with structural nonlinearity. Nonlinear Dynamics 18 (3), 289–301.

Lavergne, F., Villaume, F., Jeanneau, M., Tarbouriech, S., Garcia, G., Aug 2005. Nonlinear robust autoland. In: AIAA Guidance, Navigation, and Control Conference and Exhibit. pp. 1–16.

Lima, E., Gomide, F., Ballini, R., Sep. 2006. Participatory evolving fuzzy modeling. In: 2006 International Symposium on Evolving Fuzzy Systems. pp. 36–41.

Ljung, L., 1999. System Identification: Theory for the User, 2nd Edition. Prentice-Hall, Inc., Upper Saddle River, NJ, USA.

McFarlane, D., Glover, K., Jun. 1992. A loop-shaping design procedure using $H_\infty$ synthesis. IEEE Transactions on Automatic Control 37 (6), 759–769.

Oliveira, L., Bento, A., Leite, V., Gomide, F., 2019a. Robust evolving granular feedback linearization. In: Kearfott, R. B., Batyrshin, I., Reformat, M., Ceberio, M., Kreinovich, V. (Eds.), Fuzzy Techniques: Theory and Applications. Springer International Publishing, Cham, pp. 442–452.

Oliveira, L., Franco, A., Leite, V., Outubro 2015. Estratégia para síntese do ganho da malha de controle robusto em sistemas com realimentação linearizante via algoritmo diferencial evolutivo. In: Simpósio Brasileiro de Automação Inteligente. Natal, RN, pp. 1824 – 1829.

Oliveira, L., Leite, V., Bento, A., Gomide, F., June 2019b. Robust granular feedback linearization. In: 2019 IEEE International Conference on Fuzzy Systems (FUZZ-IEEE). pp. 1–6.

Pedrycz, W., Gomide, F., 2007. Fuzzy Systems Engineering: Toward Human-Centric Computing, 1st Edition. Wiley-IEEE Press, Hoboken, New Jersey.

Sousa, A. C. E., Leite, V. J. S., Rubio Scola, I., Sept. 2018. Affordable control platform with MPC application. Studies in Informatics and Control 27 (3), 265–274.